Nuclear Engineering and Technology 48 (2016) 434–447

Available online at ScienceDirect

Nuclear Engineering and Technology

journal homepage: www.elsevier.com/locate/net

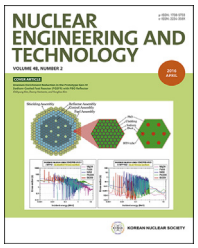

Original Article

Using Largest Lyapunov Exponent to Confirm the Intrinsic Stability of Boiling Water Reactors

Carlos J. Gavilán-Moreno [a] *and Gilberto Espinosa-Paredes* [b,*,1]

[a] *Iberdrola Generación, S.A., Cofrentes Nuclear Power Plant, Project Engineering Department, Paraje le Plano S/N, Cofrentes E46625, Valencia, Spain*

[b] *Área de ingeniería en Recursos Energéticos, Universidad Autónoma Metropolitana-Iztapalapa, México D.F. 09340, Mexico*

ARTICLE INFO

Article history:
Received 9 July 2015
Received in revised form
14 November 2015
Accepted 14 December 2015
Available online 21 January 2016

Keywords:
Attractor
BWR
Instability
Large Lyapunov Exponent
Limit Cycle

ABSTRACT

The aim of this paper is the study of instability state of boiling water reactors with a method based in largest Lyapunov exponents (*LLEs*). Detecting the presence of chaos in a dynamical system is an important problem that is solved by measuring the LLE. Lyapunov exponents quantify the exponential divergence of initially close state-space trajectories and estimate the amount of chaos in a system. This method was applied to a set of signals from several nuclear power plant (NPP) reactors under commercial operating conditions that experienced instabilities events, apparently each of a different nature. Laguna Verde and Forsmark NPPs with *in-phase instabilities*, and Cofrentes NPP with *out-of-phases instability*. This study presents the results of intrinsic instability in the boiling water reactors of three NPPs. In the analyzed cases the limit cycle was not reached, which implies that the point of equilibrium exerts influence and attraction on system evolution.

1. Introduction

Historically, the oscillatory behavior of high amplitude and frequency in the thermal power of a boiling water reactor (BWR) is referred to as a nuclear instability [1]. Even in the instability state, the system is subject to the attraction of the equilibrium point, which means it is possible to assert that the limit cycle has not been reached, and stability restoration is possible. This reasoning is consistent with the intrinsically stable condition of the reactor under commercial operating conditions. In this work, the definition of the largest Lyapunov exponent (*LLE*), which marks the stability and divergence, is used to demonstrate the abovementioned behavior.

* *Corresponding author.*
E-mail address: gepe@xanum.uam.mx (G. Espinosa-Paredes).

[1] On sabbatical leave from the Facultad de Ingeniería of the Universidad Nacional Autónoma de México through the Programa de Estancias Sabáticas del CONACyT.

http://dx.doi.org/10.1016/j.net.2016.01.002

The limit cycles that arise in BWRs was analyzed by Muñoz-Cobo and Verdu [2] using the Hopf bifurcation theory and variational methods to find the limit cycles of bifurcationing dynamical system. These authors concluded that a Hopf bifurcation takes place in BWRs when passing to the nonlinear regime region, and the results obtained with variational methods agree with the ones obtained using the Hopf bifurcation theory.

As is well known, all Lyapunov exponents from stable equilibrium points are real and negative numbers; however, for stable limit cycles, one Lyapunov exponent is zero and the rest are real and negative numbers. Therefore, BWR stability can be obtained from the Lyapunov exponents. In order to estimate the asymptotic stability domains of nonlinear reactor models, two constructive methods were described by Yang and Cho [3]. One of these methods is based on expansion of a Lyapunov function, and the other methods are based on the expansion of any positive definite function. These methods were established on the stability definitions of Lyapunov itself. The method based in expansion of a Lyapunov function provides a sequence of stability regions that eventually approaches the exact stability domain, but requires many expansions to obtain the entire stability region because the starting Lyapunov function usually corresponds to a small stability region and because most reactor systems are stiff.

Muñoz-Cobo et al. [4] proposed a methodology to obtain reactor stability from Lyapunov exponents using dynamic reconstruction techniques and the algorithm based on the work of Eckmann et al. [5]. The methodology was applied to computer-generated signals obtained with the model of March-Leuba [6], where the estimations of higher Lyapunov exponents are close to the real.

When one applies the algorithm given by Eckmann et al. [5] to signals from systems such as BWRs with large amounts of noise, the Eckmann et al. [5] method fails to give an accurate value of the higher Lyapunov exponents. A methodology based on Eckmann et al.'s [5] idea to compute the LLEs in real systems with large amounts of noise was developed by Pereira et al. [7]. This methodology was applied to Average Powerrate Monitor (APRM) signals from Cofrentes Nuclear Power Plant (NPP) and the different levels of noise with the Mareh-Leuba [6] model. When this methodology applies the AR modeling, the determination of Lyapunov exponents in linear stability regime cannot be applied when the system enters into nonlinear regime (e.g., limit cycle conditions).

The dynamic reconstruction techniques were applied by Verdú et al. [8] to BWRs with a large amount of noise. These authors adapted a technique for short and noisy data sets based on a global fit of the signal by means of orthonormal polynomials, which was applied to the analysis of the neutronic power signals to characterize the stability regime of BWR reactors. The method works well for simulated noisy signals; however, for the experimental signals from Ringhals 1 BWR, the reconstructed phase space for the system is not appropriate—here, it was necessary to apply a modal decomposition treatment for the signals, producing signals with better behavior.

A theory of stochastic bifurcation in the vicinity of power oscillation in BWRs was developed by Konno et al. [9]. According to these authors, the deterministic Hopf bifurcation is destroyed by the incorporation of noise in the sense that the Lyapunov exponent of the system is always negative in any case near the onset of power oscillation, and the values of decay ratio always take a value less than 1.

The slope of the correlation integral (SOCI) gives the information dimension for a certain value of the resolution, which as a whole forms a continuous spectrum that allows researchers to investigate the dynamics accordingly as the resolution changes [10]. SOCI was applied to the Forsmarks BWR stability benchmark [11], and according to the results, SOCI can be an alternative stability indicator and can complement the decay ratio.

Castillo et al. [12] developed a consistent method to verify the existence of limit cycles in a BWR, which was used for the analysis of APRM signals with small amounts of data containing noise. These authors concluded that the use of both the dominant Lyapunov exponent method and the SOCI method, with the Savitzky–Golay filtering method, for the analysis of BWR APRM signals should be complementary to the linear methods.

Stability analysis in nuclear reactors using Lyapunov exponents was applied to study the fuel concentration [13]. The results obtained by Khoda-Bakhsh et al. [13] with the increase in fuel concentration, are as follows. (1) In the subcritical regime, the neutron population grows when the SOCI gives the information dimension for a certain value of the resolution, which as a whole forms a continuous spectrum that allows handlers to investigate the dynamics accordingly as the resolution changes increasing the fuel concentration. (2) The Lyapunov exponent takes negative values around the critical neutron population. (3) In the supercritical state, the Lyapunov exponent is positive, implying that the neutron diffusion phenomena are spatiotemporal chaos.

In their recent work, Li et al. [14] analyzed a model based on the mathematical definition of stability in the differential equation qualitative theory. These authors took into consideration a single group of delayed neutrons and power reactivity feedback. The difference between stability in the mathematical sense and in the physical sense is explained in terms of phase locus near the equilibrium point.

Unlike previous work, the definition of the greatest exponent of Lyapunov (LLE) is applied in this work to establish the *intrinsically stable condition* of three nuclear reactors under commercial operating conditions. Owing to the behavior observed in thermal power time series, attractors, and LLE time series, it is considered that the system has a reversible nature tending to equilibrium. In the analyzed cases, the limit cycle was not reached, which implies that the point of equilibrium exerts influence and attraction on system evolution. In this work, we present the results obtained for the overall LLE value of the complete thermal power time series, and its evolution in time, LLE(*t*).

This study proposes to avoid calling the situations analyzed as *unstable state* or *instability*, as well as to use the expression *divergent power evolution*, which refers to its evolutionary nature. It also justifies the reversibility of the reactor and its ability to return to a stable state, favored by the negative trend of the LLE time series, which causes the system to have negative LLE values and stable status.

2. Preliminaries

Let us suppose a stable system consisting of a mass m that revolves around another mass M, e.g., a planetary system, and also imagine that the central point is fixed. The mass m revolves around the mass M with linear and tangent speed V, which means that centrifugal acceleration compensates for gravitational attraction acceleration. To make the case more realistic, suppose that mass m is not constant and varies randomly around its average value. In such a case, the real movement will not be a line, but a band in which the position will be random, as illustrated in Fig. 1.

Let us imagine now that a particle of mass m is subjected to a centrifugal acceleration change resulting from module alterations in tangential speed V. This will cause an orbit and radio change based on speed alterations. The orbit will stop being a circular strip to become a spiral strip, in which the center will still be mass M. This situation would continue until speed V module exceeds the so-called escape value, time in which the path is a tangent line to the last position on the spiral (Fig. 2).

The first two states are stable (Fig. 1), and the last one is described as unstable and generator of an out-of-reach trajectory gravitational center action (Fig. 2). If speed increase ceases, there are two possibilities. First, when the speed is frozen in the last value then, a new orbit and stable state are established. Second, if the system is dissipative and the tangential speed returns progressively to its initial value. The system will then describe a convergent spiral orbit toward the initial orbit, for a stable baseline to occur.

Taking an orbit-oriented approach, the case described is easier and more intuitive. In a steady state, an n orbit and $n+1$ orbit are identical, which implies that the distance between them tends to be zero. In a divergent state or transition, the

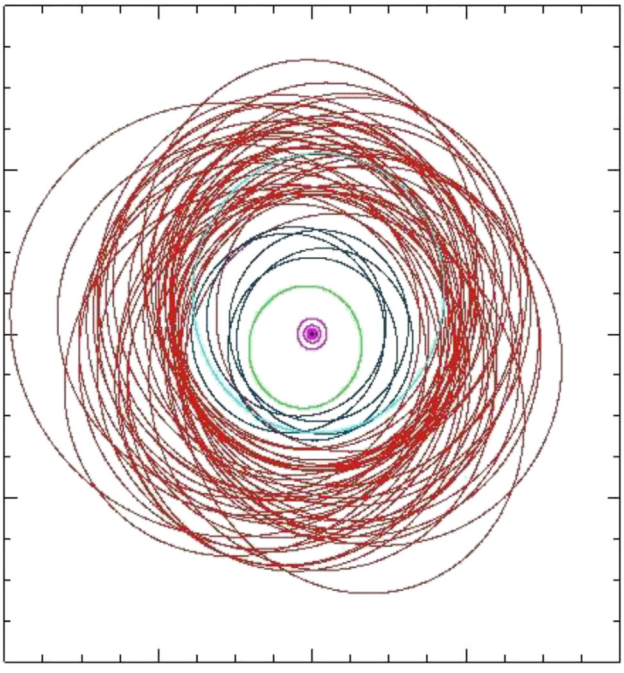

Fig. 1 – Irregular orbits.

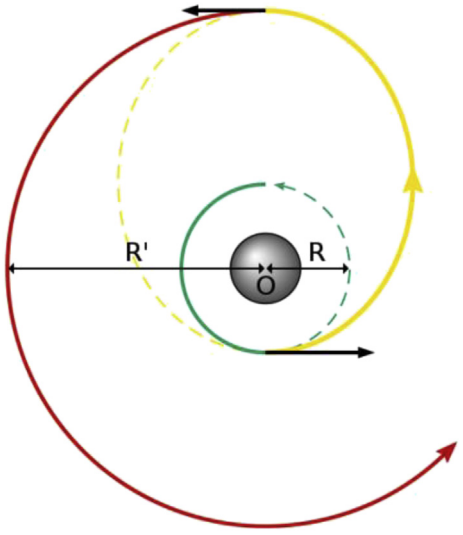

Fig. 2 – Stable orbits, divergent orbits, and limit cycle.

$n+1$ orbit is significantly greater than the n orbit, meaning their distance will be positive and greater than zero. In the case of the so-called out-of-control state, the $n+1$ orbit is far from the n orbit in a value tending to infinity.

Systems studied, in nature and industry, are normally nonlinear, although they may be simplified or linearized in some sections. The case study involves a BWR—, a nonlinear, chaotic, and stationary system [15]. Nonlinear, dynamic systems have a chaotic behavior characterized by small variations in initial conditions that after a period of evolution have a very different impact on the system. This divergent system behavior in relation to neighbor states can be quantified using Lyapunov coefficients—useful to estimate if the system tends to the point of attraction or equilibrium, remains in a stable orbit, or evolves to a point of no return and out of control.

Now, these concepts relative to orbits, dynamic and chaotic systems, are applied to the BWR thermal power time series. If orbits exist, it is necessary to generate their space by exploring and determining the attractor that generates entities in phase space and therefore transforms time series into a three-dimensional figure (Section 5.5). This allows transformation of the time series into a set providing information on system status and evolution. The system, a BWR, has an evolution conditioned by the described orbits.

Once orbits are obtained, Lyapunov coefficients are defined and calculated by taking two consecutive orbits, as illustrated in Fig. 3.

We also consider two points represented as X_0 and $X_0 + \Delta X_0$, and establish the distance of two orbits as $\Delta X(X_0, t)$. The behavior of function $\Delta X(X_0, t)$ will be as follows: (1) in a system with attraction points or stable orbits, the value of $\Delta X(X_0, t)$ decreases asymptotically in time or with the number of orbits, which tend to converge; and (2) if the system is divergent, the value of $\Delta X(X_0, t)$ will increase exponentially, with a spiral behavior.

In order to establish a comparison parameter, the Lyapunov coefficient is defined as follows:

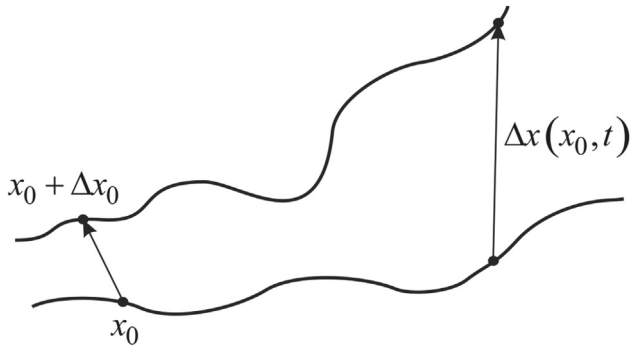

Fig. 3 – Graph of two orbits and their characteristic parameters.

$$\lambda = \lim_{\substack{t\to\infty \\ |\Delta X_0|\to 0}} \frac{1}{t} \ln \frac{|\Delta X(X_0, t)|}{|\Delta X_0|} \tag{1}$$

The interpretation of λ and its values is as follows. For values of $\lambda < 0$, the orbits are attracted by a fixed point or a stable orbit. These negative values of the Lyapunov coefficient define a dissipative—not a conservative—system (i.e., damped harmonic oscillator) characterized by its asymptotic stability. System stability will increase as coefficient negativity augments. For values of $\lambda = 0$, the orbit corresponds to a neutral point, implying that the system is in a permanent steady state. In such cases, the system is considered conservative and orbits maintain constant separation. For values of $\lambda > 0$, the system and orbits are clearly divergent. Nearby orbital points, regardless of their proximity, diverge to any value of separation.

Fig. 4 shows examples of orbits of systems with negative and null Lyapunov coefficient.

This work focuses on large Lyapunov exponent (*LLE*) as they determine system instability. Several methods or algorithms are used to calculate LLE in a time series (e.g., [5,16,17]). In this work, the ideas from the work Rosenstein et al. [17] were applied.

3. Dynamics power generation BWR

The thermal power time series selected correspond to three instabilities of different primary source in three NPPs in operation: Cofrentes NPP (Spain); Laguna Verde NPP (Mexico); and Forsmark NPP stability benchmark (Sweden).

Fig. 5 corresponds to the Cofrentes nuclear power station instability, which occurred on January 29, 1991 during the startup sequence after an emergency trip. At the time of the incident, the plant had a thermal power of 41% with a flow rate of 38%, conditions in which the thermal power oscillations occurred. They were controlled by the operators through control rod insertion. The instability, considered *out-of-phase*, was caused by feedwater temperature reduction.

Fig. 6 corresponds to the Laguna Verde (Veracruz, Mexico) nuclear power station instability event that occurred on February 24, 1995 (Table 1). Reactor 1 of Laguna Verde NPP experienced power oscillations during startup. When instability occurred, the unit had a thermal power of 35% and a core flow rate of 38%, with recirculation in low-speed and flow control valves (FCVs) partially open. When the anomaly was detected, the operator opened the FCVs causing an increase in core flow rate and an oscillation decrease until stability was reached again. In any case, the operator decided to manually shut down the reactor. This instability was considered as *in phase*.

Fig. 7 represents the case of Fosmark NPP, which is different because it is not a power instability caused by plant operation, but a premeditated situation. Thus, the data range used correspond to the "Nuclear Science Committee of the OECD Nuclear Energy Agency (NEA)" project intended to compare different signal analysis methods for BWR stability studies [11]. The instability, categorized as *in phase*, was caused by operation within the power-flow map instability area.

The sampling frequency and the duration of each event described are reflected in Table 1.

4. Methodology

This section describes the general LLE calculation process and the construction of its time series, which is used to analyze thermal power evolution and instabilities. Once calculations are finished, the analysis phase begins with the aim of comparing the LLE time series to the thermal power evolution, and the LLE sign to the instability starting moment of each reactor.

The LLE calculation (for a short time series), described by Rosenstein et al. [17], is performed on the short and stationary time series. LLE is defined as:

$$d(t) = Ce^{\lambda_1 t}, \tag{2}$$

where $d(t)$ is the average divergence at time t and C is a constant that normalizes the initial separation. From the definition of λ_1, one can assume that the j^{th} pair of nearest neighbors diverge approximately at a rate given by the LLE. Then,

$$d_j(i) \approx C_j e^{\lambda_1 (i\Delta t)} \tag{3}$$

The approach for calculating λ_1 is given by Sato et al. [18]:

$$\lambda_1(i) = \frac{1}{i\Delta t} \frac{1}{(M-i)} \sum_{j=1}^{M-i} \ln \frac{d_j(i)}{d_j(0)}, \tag{4}$$

i.e., a method that tracks the exponential divergence of nearest neighbors. In this expression, Δt is the sampling period, $d_j(i)$ is the distance between the j^{th} pair of nearest neighbors after i discrete time steps ($i\Delta t$), and M is related to reconstruction delay, embedding dimension, and point of time series.

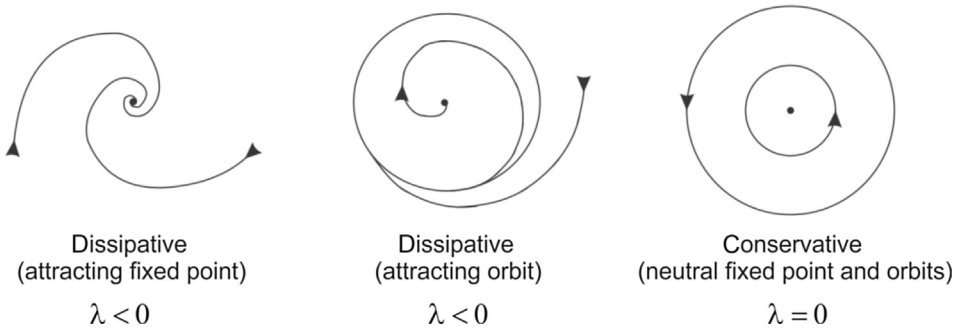

Fig. 4 – Example of orbits and characteristic: Lyapunov exponents.

The initial distance from the j^{th} point to its nearest neighbor, $d_j(0)$, is calculated as [17]:

$$d_j(0) = \min_{X_j} \left\| X_j - X_{\widehat{j}} \right\|, \quad \text{for} \quad \left| j - \widehat{j} \right| > \text{mean period}, \tag{5}$$

where $X_{\widehat{j}}$ is the nearest neighbor and X_j is the reference point. The *mean period* is given in Table 2.

In this work, two cases were analyzed for each dynamics power generation series: Case A, LLE is obtained for the complete thermal power time series of each reactor; and Case B, LLE is obtained for every moment. The rolling window methodology is applied in order to establish an LLE time series.

The methodology to determine LLE considers the following main steps. Step 1. Reconstructing of the attractor dynamics from single time series, in order to identify the main parameters. Step 2. Determination of *main period* (Δt). The main period was applied with fast Fourier transform to the signals. Step 3. Determination of *reconstruction delay* (J), which was calculated using the average mutual information method. Step 4. Selecting of embedding dimension (m). We applied the False Nearest Neighbors (e.g., [19,20]). Step 5. Description of attractor characteristics. With the parameters Δt, J, and m described in Steps 2–5, we obtain the attractors. Step 6. LLE is calculated using Eqs. (3)–(5) for Cases A and B, where $M = N - (m-1)J$.

The methodology used to determine rolling window and subset sizes will be developed in Section 6.2.

5. Developed

5.1. *Reconstructing the attractor dynamics*

The first step of the approach involves reconstructing the attractor dynamics from single time series. In this work, the method of delays was applied. The reconstructed trajectory, $\mathbf{X}$, can be expressed as a matrix: $\mathbf{X} = (X_1, X_2, \ldots, X_M)^T$, where each row is a phase-space vector, and X_i is the state of the system at discrete time i. For an N-point time series, $\{x_1, x_2, \ldots, x_N\}$; each X_i is given by:

$$X_i = \left(x_i\ x_{i+j} \ldots x_{i+(m-1)J}\right), \tag{6}$$

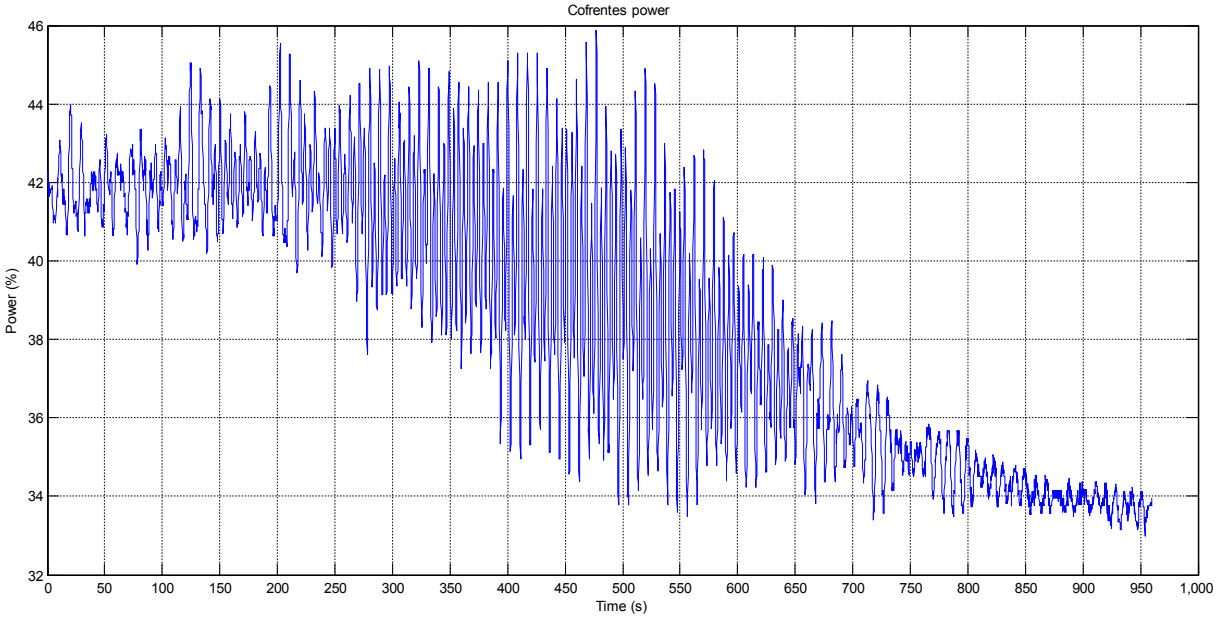

Fig. 5 – Cofrentes instability event.

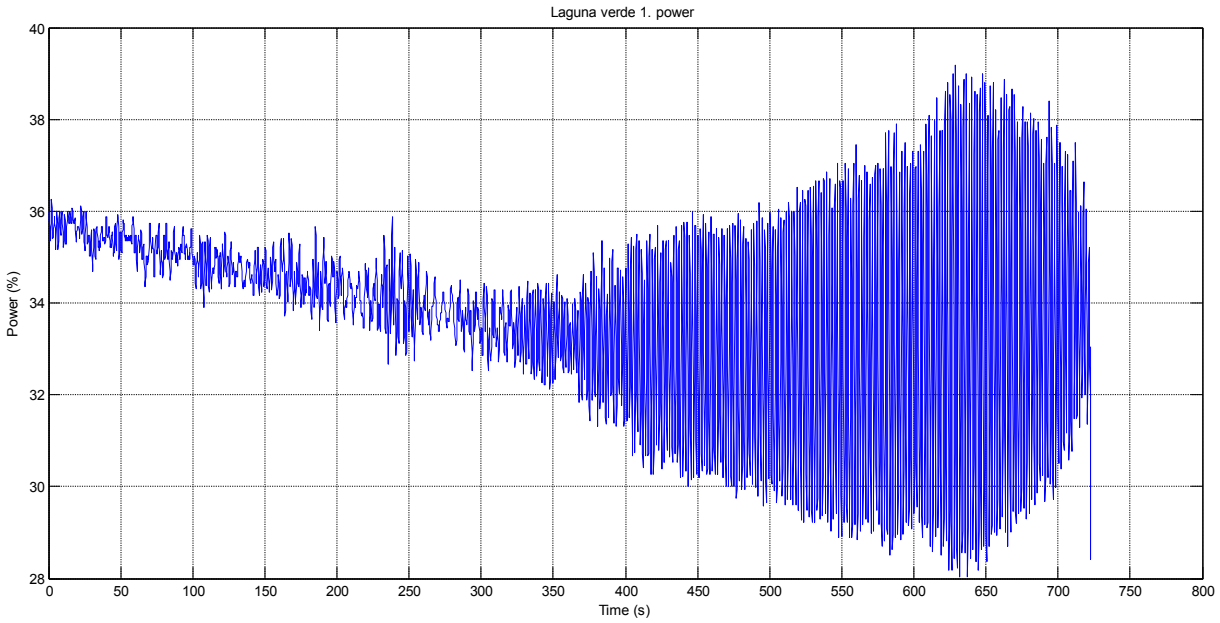

Fig. 6 – Laguna Verde instability event.

where J is the *reconstruction delay* and m is the *embedding dimension*. Then, $\mathbf{X}$ is an $M \times m$ matrix, and m, M, J, and N are related as: $M = N - (m-1)J$.

5.2. *Main period (Δt)*

The main period was applied using fast Fourier transform to the signals shown in Figs. 5–7. The main period values are shown in Table 2.

Period and frequency information shown in Table 2 corresponds to the main value and is present in the entire thermal power time series. Values are consistent with the instability state (e.g., [21–24]).

5.3. *Reconstruction delay*

Reconstruction delay (J) is calculated using the average mutual information method, and is the value of T, where the following function is minimized:

$$I_d(J) = \sum_{n=1}^{N} P(x_n, x_{n+J}) \cdot \log_2 \frac{P(x_n, x_{n+J})}{P(x_n) \cdot P(x_{n+J})}, \quad (7)$$

where $P(x_n)$ is the probability of observing x_n and $P(x_n + x_{n+J})$ is the probability of observing both values. Reconstruction delay values obtained for this analysis are shown in Table 3.

Table 1 – Identifying characteristics of each analyzed signal.

NPP Time series	Duration (s)	Sampling period (s)[a]
Cofrentes	250	0.05
Laguna Verde U1.	700	0.2
Forsmark	320	0.08

NPP, nuclear power plant.
[a] The sampling period (Δt) is applied in Eq. (3) for complete time series.

5.4. *Embedded dimension (m)*

Imagining a dynamic, stationary, and deterministic system observed through a function such as:

$$g : M \to R; g(\cdot) : z_n \to x_n = g(z_n), \quad (8)$$

a scalar magnitude will be obtained at any time. This scalar value does not offer a full system description, which can be obtained by observing x_n many successive times. According to the Takens embedding theorem [25,26], if a number denominated m is sufficiently large, the evolution of $(x_n, x_{n+1}, \ldots, x_{n+m})$ will be the same as z_n. Then, Takens theorem giving conditions under which a discrete-time dynamical system can be reconstructed from scalar-valued partial measurements of internal states.

In general, the aim of selecting an embedding dimension is to make a sufficient number of system state observations to solve the deterministic system state unambiguously.

As for the methodology to calculate m, we applied the False Nearest Neighbors (e.g., [19,20]). Then, the embedding dimension is obtained as the minimum value n that satisfying the following condition:

$$\frac{\left|x_{t-(n+1)J} - x_{t'-(n+1)J}\right|}{v_t - v_t^{NN}} > R_T \quad (9)$$

where

$$v_t = (x_{t-J}, x_{t-2J}, \ldots x_{t-nJ}) \quad (10)$$

$$v_t^{NN} = (x_{t'-J}, x_{t'-2J}, \ldots, x_{t'-nJ}) \quad (11)$$

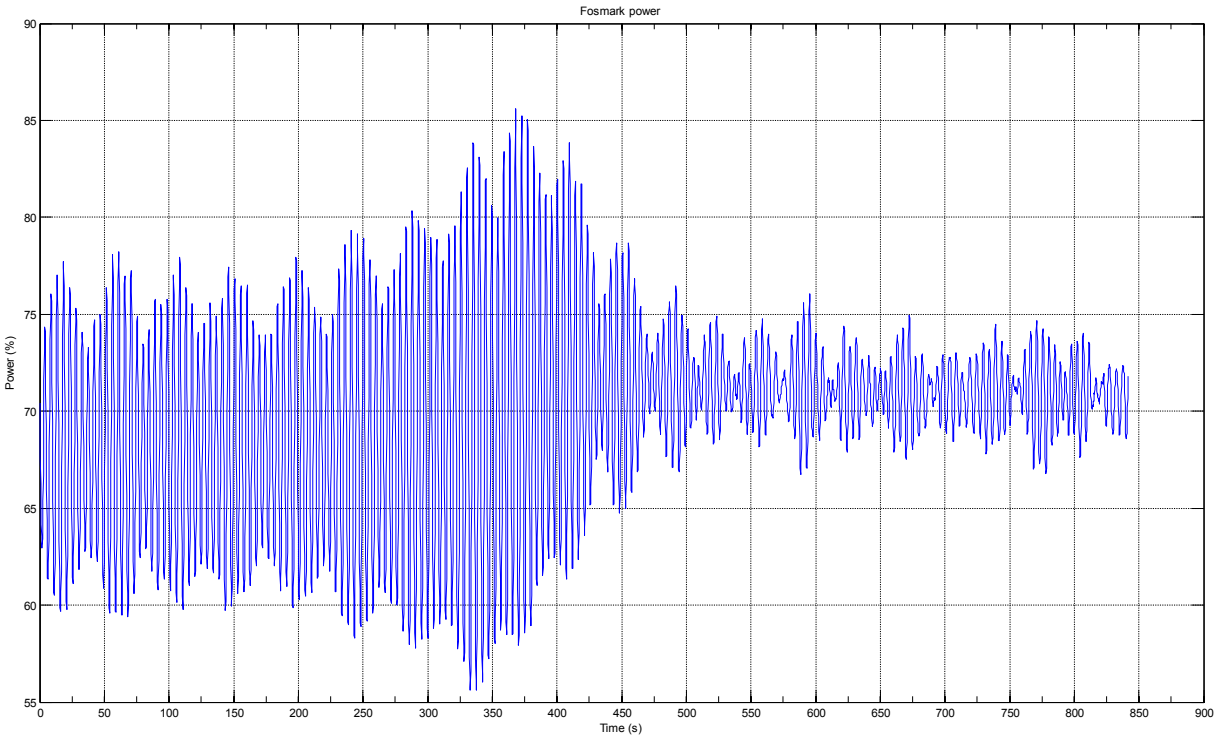

Fig. 7 – Forsmark stability benchmark: APRM signal, case c5-aprm1 [11].

that is considered the nearest neighbor. In this expression, R_T is the criterion for the nearest false neighbors. Calculation of the embedded dimension requires knowing the reconstruction delay (J) value, which is given in Table 3. The results calculated by the mutual information method are presented in Table 4.

5.5. *Attractor characteristics*

The vectors that reconstruct the state space of the system is given by Eq. (6), where the reconstruction delay (J) and embedded dimension (m) are given in Tables 3 and 4, respectively, for each NPPs. This work uses the fractal nature of neutronic power signal (time series) in BWRs. This fractal nature of the BWR thermal power signal leads to the creation of attractors for three neutronic power time series in three different reactors under unstable conditions. The attractor morphology and characteristics help us to analyze the stability, instability, and reversibility.

Typically, graphic representation is difficult with those dimensions, so reduction should be necessary from the vector dimension to three dimensions, to visualize the attractor. In order to represent attractors, in a three-dimensional space, it is necessary to generate a list of x, y, and z coordinates so that points can determine the orbits and the attractor [27,28].

Table 2 – Frequency and main period (Δt).

NPP time series	Frequency (Hz)	Δt (s)
Cofrentes	0.4707	2.1244
Laguna Verde U1	0.5382	1.8580
Forsmark	0.5286	1.8917

NPP, nuclear power plant.

Based on the definition of attractor, the y and z coordinates are delayed coordinates from the same series: $y(t) = s(t + J)$ and $z(t) = s(t + 2J)$. Taking into account the J values, the attractors are presented in Figs. 8–10.

An analysis of Figs. 8–10 leads to the conclusion that the attractor, at least in 3D, is a fully developed three-dimensional structure. A detailed analysis shows that the attractor is a divergent hyperbolic cone. Cone divergence or diameter increasing is related with instability progression and is correlated to power variation increase. Similarly, it can be determined that orbits comprising the attractor are within the so-called limit orbit, meaning the system remains attracted by the cone's central axis or point. This is shown in Fig. 8 as instability is corrected and returned to a stable condition.

6. Results and discussion

In Section 4, the methodology of LLE calculation in a time series was reviewed and explained, and in Section 5 the development is presented. The effectiveness of LLE has been demonstrated in previous works for different applications (e.g., [29–36]).

In this section, LLE results will be presented for two cases: Case A. LLE is obtained for the complete thermal power time series of each reactor, and Case B. LLE is obtained for every moment for each reactor, i.e., as function of time, LLE(t).

6.1. *Case A. Full thermal power time series characterization*

First, the complete time series of the LLE was determined to fully characterize reactor behavior over the analyzed period.

Table 3 – Reconstruction delay (J).

Time series of NPP	No. of events	J(s)
Cofrentes	7	0.35
Laguna Verde U1	2	0.4
Forsmark	5	0.4

No., number; NPP, nuclear power plant.

Table 5 shows the complete time series values of LLE. In this case, LLE was obtained using the data from Table 1.

The LLE values shown in Table 5 are positive, meaning that the system defined in Section 2 is diverging. The behavior is nonpersistent, an interpretation that is consistent with the divergent form of the attractor (Figs. 8–10).

6.2. Case B. LLE obtained for every moment for each reactor

Once the overall performance is analyzed, it is necessary to investigate temporal LLE behavior and system evolution. The proposed rolling window scheme is intended to determine the following short time series:

$$(x_i, x_{i+1}, \ldots, x_{i+n}), \quad \text{for } i = 1, 2, \ldots, \ell - n, \tag{12}$$

where ℓ is time series length. The short time subseries have to be stationary for an LLE value to be calculated using the same methodology of the full neutronic power time series. The result of this process will be a pair (i, LLE(i)) and therefore an LLE time series.

The objective is to determine the minimum number n in Eq. (12) for a stable representative LLE and a stationary thermal subseries. To calculate the value of n, the approach used to obtain the Hurst exponent in previous studies is used [10]. This approach establishes that to calculate the value of n, it is necessary to satisfy:

$$\frac{d(LLE)}{dn} = 0 \tag{13}$$

With this aim, we will calculate LLE with various values of n, starting from the origin to $n=\ell$. The selected window values are presented in Table 6.

Using the calculated window length shown in Table 6, in a rolling window scheme, the LLE time series is shown in Figs. 11–13 for every analyzed NPP. The parameters to be analyzed are values, trends and sign changes, intervals of homogeneous tendency, and correlations with maneuvers, as well as autonomous reactor behaviors.

The analysis criteria that were applied in this study are as follows: (1) LLE < 0 indicates a stable reactor situation, (2) LLE > 0 indicates a situation in which orbits are slightly divergent, is the much higher value of LLE, (3) the existence of a positive trend implies a reactor drift and the existence of a destabilizing event. This means the system (reactor) moves away from its equilibrium point, and (4) if the trend is negative, the system will reverse the evolution and converge toward the equilibrium point.

Table 4 – Integration dimension values.

NPP time series	Embedded dimension (m)
Cofrentes	6
Laguna Verde U1	6
Forsmark	4

NPP, nuclear power plant.

6.2.1. Cofrentes NPP

As shown in Section 3 and in Fig. 11, the plant was starting up after a reactor trip. The first interval to be studied is between the origin and the value of 60 seconds. In this interval, the plant does not have detectable instability but the value of LLE is not negative, meaning instability was present but not evident. The analysis of Fig. 11 reveals that during the interval from instant $t = 60$ seconds to moment $t = 450$ seconds, thermal power causes an oscillation amplitude increase. The LLE value and tendency are clearly positive, with LLE coinciding the most with the moment of maximum amplitude. Between $t = 450$ seconds and $t = 600$ seconds, the operator inserted control rods, causing an oscillation decrease, stabilization, and subsequent power reduction. In that same interval, LLE tendency is clearly negative and takes the series to the negative half-space.

LLE trend and value indicate thermal power reactor status. The interesting thing about LLE time series is what happens between the initial state and the timing of control rod insertion between $t = 0$ and $t = 450$ seconds, when the system evolves autonomously without human action.

Fig. 11 (upper) shows that in the interval between 0 and 450 seconds, the LLE time series behavior has the appearance of sawteeth, with a succession of maximums and minimums. The LLE time series form indicates that the system reacts to cancel the original state and mechanism of divergence (instability). Thus, each maximum, representative of a destabilizing mechanism, is followed by a minimum, indicative of the existence of internal mechanisms tending to stabilize the system.

6.2.2. Laguna Verde U1 NPP

The thermal power time series (Fig. 12) is apparently stable up to $t = 320$ seconds. Prior to that time, at about $t = 240$ seconds, an event of high local amplitude (a forerunner of further instability) is registered [15]. In the LLE time series, the values are negative but the trend rises, with episodes of positive values in $t = 240$ seconds and $t = 320$ seconds.

In the interval between $t = 320$ seconds and $t = 420$ seconds, the signal seems to saturate, with high but constant amplitude. In the same interval, the LLE time series returns to negative values. From $t = 420$ seconds, amplitude is increased significantly, as well as the LLE value, with a rise to the positive half-space and maximum values being reached.

After $t = 600$ seconds, following FCV opening, amplitude decreases and thermal power tends to stabilize. During this same period, the LLE presents a sustained negative trend bringing value to the seminegative space.

In the analysis of the LLE time series (Fig. 12, lower), there are peaks hovering around $t = 240$ seconds and one very

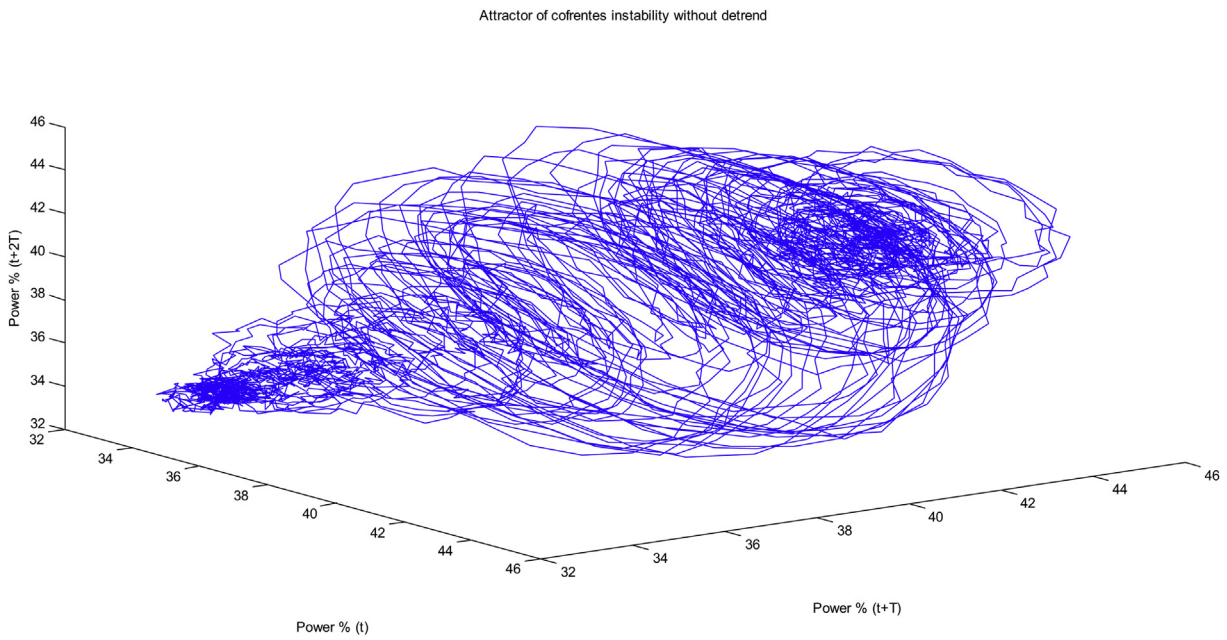

Fig. 8 – Attractor of Cofrentes Nuclear Power Plant.

distinct peak around t = 320 seconds, confirming the moment of divergence appearance (instability) in thermal power signal.

Once the coherence between LLE time series and thermal power time series is analyzed, system evolution in the autonomous divergence phase needs to be examined. To do this, the intervals between 240–320 seconds and 320–600 seconds are evaluated as that is when the system evolves independently. In both intervals, the system (BWR) evolves in two different ways. After t = 240 seconds, the operator moves the recirculation FCVs, resulting in a temporary tending to system destabilization as thermal power reaction needs to be considered. Likewise, LLE peaks around 240 seconds, although it remains in negative values. From 240 seconds to 320 seconds, the LLE series trend is clearly positive, with a behavior marked by a succession of peaks and valleys. The peaks are of positive value, whereas the valleys are in the negative semispace, meaning the system refuses to leave the stable state and fails to initiate the process of divergence (instability). From the interval between t = 320 seconds and t = 600 seconds, the LLE time series has a constant positive trend and goes from the negative semispace to the positive semispace. As in the previous case of Cofrentes NPP, the behavior continues to be characterized by a graph in the form

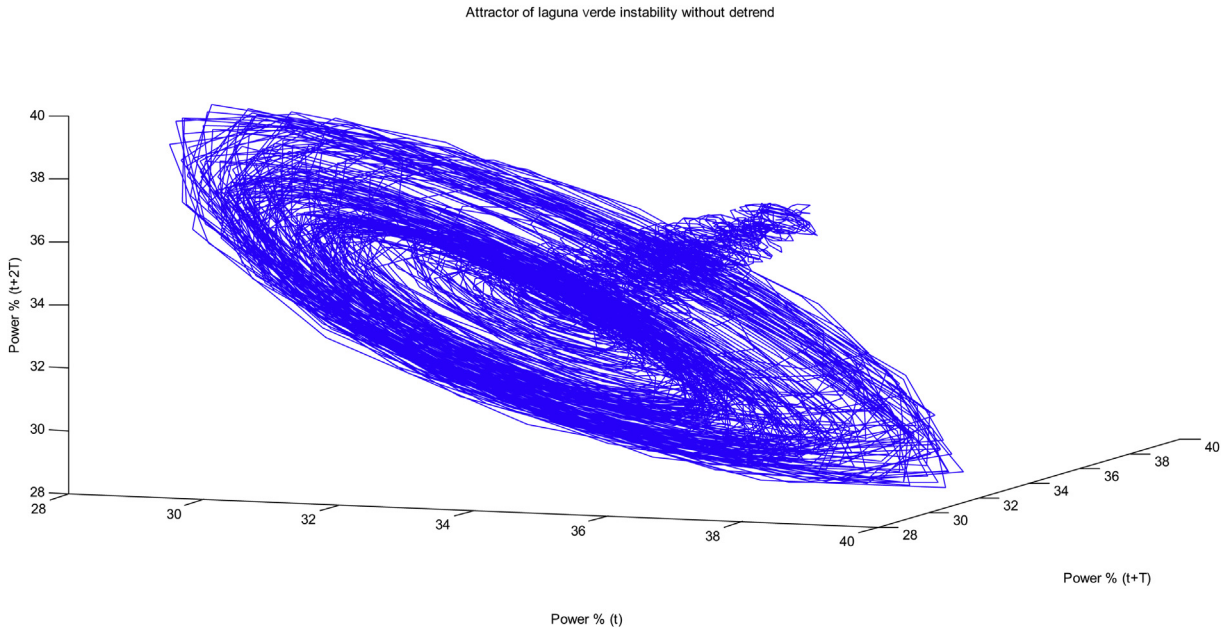

Fig. 9 – Attractor of Laguna Verde Nuclear Power Plant.

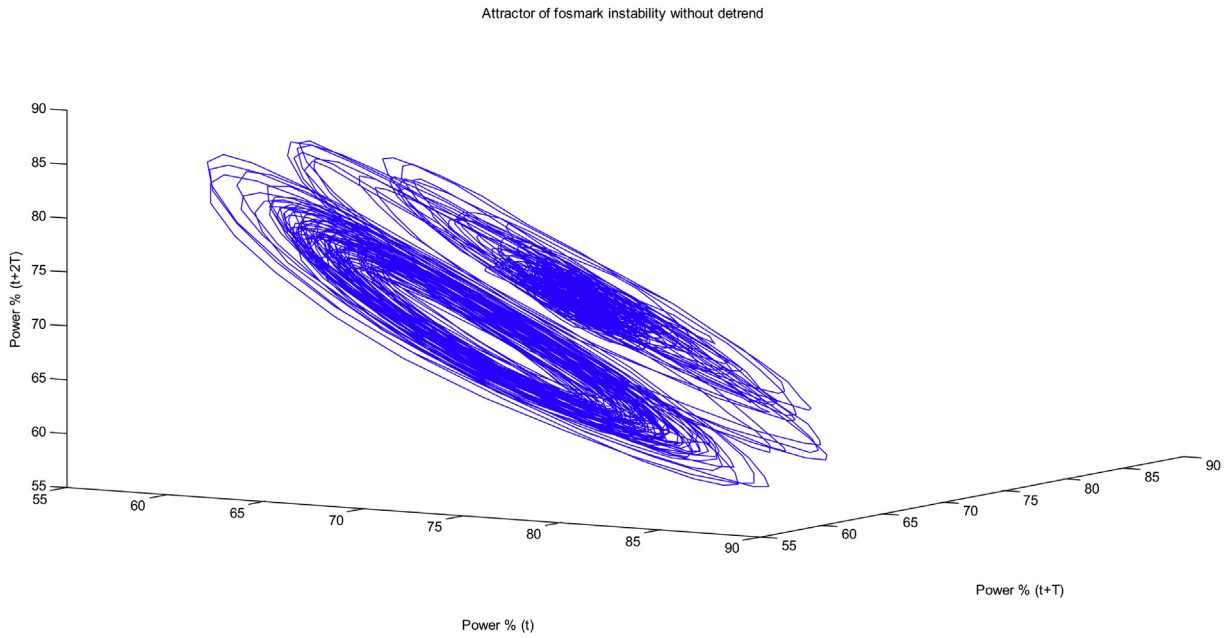

Fig. 10 – Attractor of Forsmark Nuclear Power Plant.

of sawteeth, and the system attempts to recover the equilibrium via its internal mechanisms up to $t = 550$ seconds. From that moment until $t = 600$ seconds, the operator moves the recirculation control valves, after which the internal hydraulic mechanisms begin to bring the reactor to an equilibrium point, as deduced from thermal power amplitude reduction.

6.2.3. *Forsmark NPP*

This case is not analogous to the one above as instability is raised and maintained artificially. The system is divergent (unstable), and there is no transition or evolution from an equilibrium point or stable system. The registered series is unstable along its entire length and has two different levels of amplitude (Fig. 13). Analyzing the LLE value in the entire range, it is observed that there are also two value levels: the first value corresponds to the thermal power time series part with high amplitude and the second corresponds to the low amplitude part. The LLE time series also has a transition area, similar to the power series for the interval between $t = 300$ seconds and $t = 450$ seconds, where a positive trend leads LLE to a higher positive value. Amplitude increases are preceded by a local maximum of the LLE value.

The analysis of Fig. 13 (lower) reveals that all LLE values are in the positive semispace, a situation consistent with the unstable state of the system. The sawtooth behavior described above is also observed. In the case that concerns us, wherein there is a lower thermal power signal maximum, a peak occurs in the LLE time series. Likewise, when the amplitude is maximum, the LLE marks a minimum and amplitude decreases.

It can be deduced that the LLE is an indicator of system behavior and response, valid to monitor forces tending to system destabilization (stabilization). By contrast, a valley or a minimum LLE value shown during a divergence causes the system to react and attempt to reach a point of equilibrium.

Finally, note that under these autonomous conditions, both the LLE and power series are bounded. Considering the LLE series with values between 0.2 and 0.5, as well as the shape of the attractor (Fig. 10), it is possible to conclude that the system is not unstable but diverging.

Table 5 – Complete time series values of LLE.

Time series (NPP)	LLE
Cofrentes	0.1943
Laguna Verde U1	0.1200
Forsmark	0.2400

NPP, nuclear power plant.

6.3. *Reversibility: Limit cycle*

Once the LLE time series of values with the highest Lyapunov coefficient (LLE) are calculated, it can be observed that in instability and increased amplitude situations, the LLE has positive values. On a strict interpretation, positive LLE values indicate that orbits differ from one another and the system is divergent. Taking into account both time series (Figs. 11–13) and the attractor presented in Section 5.5, it is necessary to clarify the previous interpretation because Perron's effect, which is indicative of positive LLE, is not always associated with chaos and instability. This means reversibility is possible.

Attractor behavior and reactor response show an evidence, controlled divergence, because under instability conditions, the attractor has a divergent spiral that does not surpass the cycle limit. In addition, it is clear that there are zero and negative values in the LLE time series, even in areas traditionally considered unstable. Also, power thermal time series attractors and orbits have a central point acting as gravitational center. In none of the identified cases are these orbits beyond equilibrium point attraction. Thus, the positive LLE

Table 6 – Rolling window length.

Time series NPP	Window length (n)	Time covered by the window (s)
Cofrentes	300	15
Laguna Verde U1	75	15
Forsmark	200	16

NPP, nuclear power plant.

value produces a divergent drift in attractor and orbital forms, although the reactor does not reach the limit cycle/orbit limit. This implies that the system is divergent but reversible, because the disappearance of the impulse leading to divergence causes the system to stabilize, favored by the attraction point (equilibrium point).

Another important feature is that the tendency of the LLE series at intervals of instability in the three cases analyzed is null (i.e., LLE series oscillates around the null value). It is observed that each rise in the value of LLE is followed by a decrease in the same magnitude (sawtooth). This behavior is typical of the systems with negative feedback because a variable increase augments canceling mechanisms and returns the system to its original state. Therefore, it is possible to confirm that the real system analyzed (Reactor BWR) follows the behavior described in by the United States Nuclear Regulatory Commission [21].

The reactor is a system whose nonlinearities cause oscillations to be bounded by the limited orbit. Exceeding orbit limits would result in an attraction loss at the center point of the attractor. Once the system loses attraction from the center, its behavior changes and thermal power fluctuations become aperiodic, with greater amplitudes than those shown when the system orbited in the attractor. The analyzed cases (Cofrentes, Laguna Verde, and Forsmark NPPs) follow the dynamics of two main behaviors. (1) When the system is stable and a disturbance occurs, the reactor becomes unstable linearly, power begins to grow, and a growing spiral appears in the phase space (attractor). Initially, the perturbation is small and the reactor response is linear. In this state, the LLE is going to take a positive value and its temporal evolution will have a positive average slope. (2) As oscillation grows, system nonlinearities become increasingly relevant and act as a power sink. Thus, power uprate increases the negative feedback to the reactivity and generates a negative reactivity trend. Under these circumstances, the reactor tends to subcriticality and therefore dampens oscillations, drifting to the initial equilibrium point. So, within a specific margin, the system is reversible as disturbance elimination under these conditions allows nonlinear forces to return the system to equilibrium. In this situation, the LLE in the time evolution has a negative slope and takes the system to a state of negative LLE value.

The behavior described is shown in Figs. 11–13, which correlates to the earlier phases in the time-based LLE evolution.

7. Conclusions

The LLE value on a time series is an indicator of system instability. Also, in view of Table 5, instability severity can be assessed in such a way that the more severe and prolonged

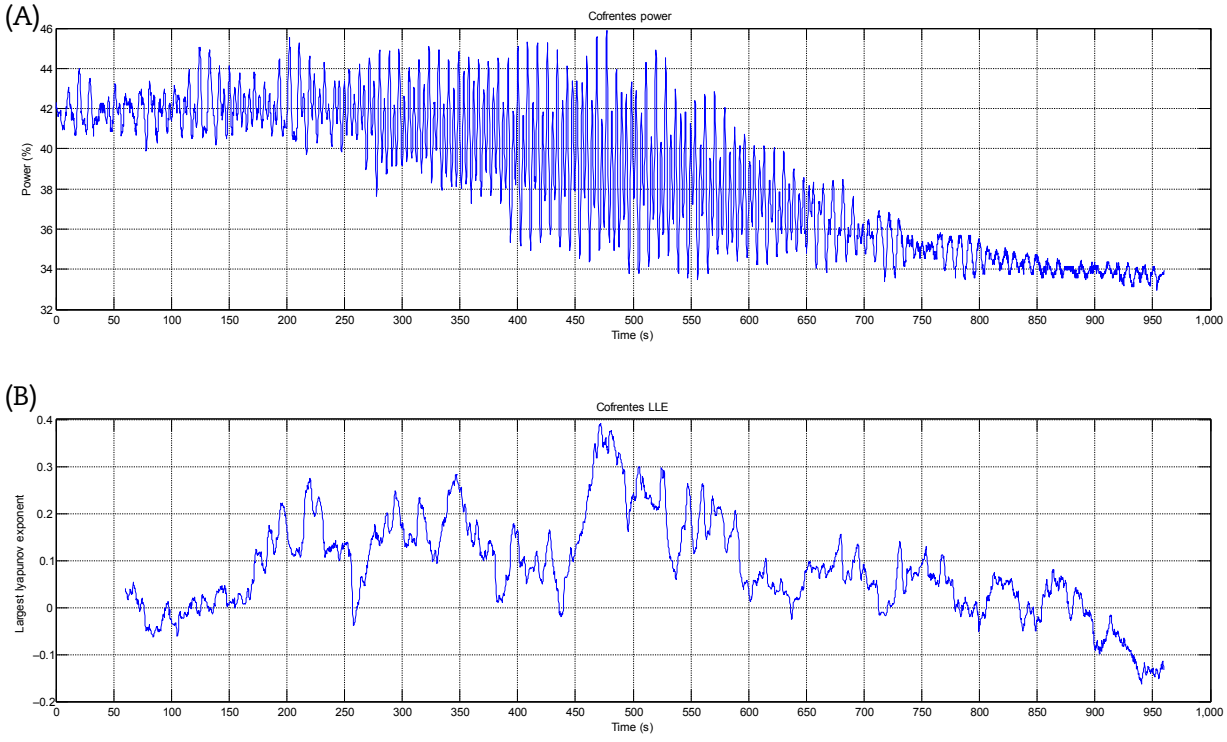

Fig. 11 – Cofrentes nuclear power plant. (A) Neutronic power series; and (B) LLE(t). LLE, largest Lyapunov exponent.

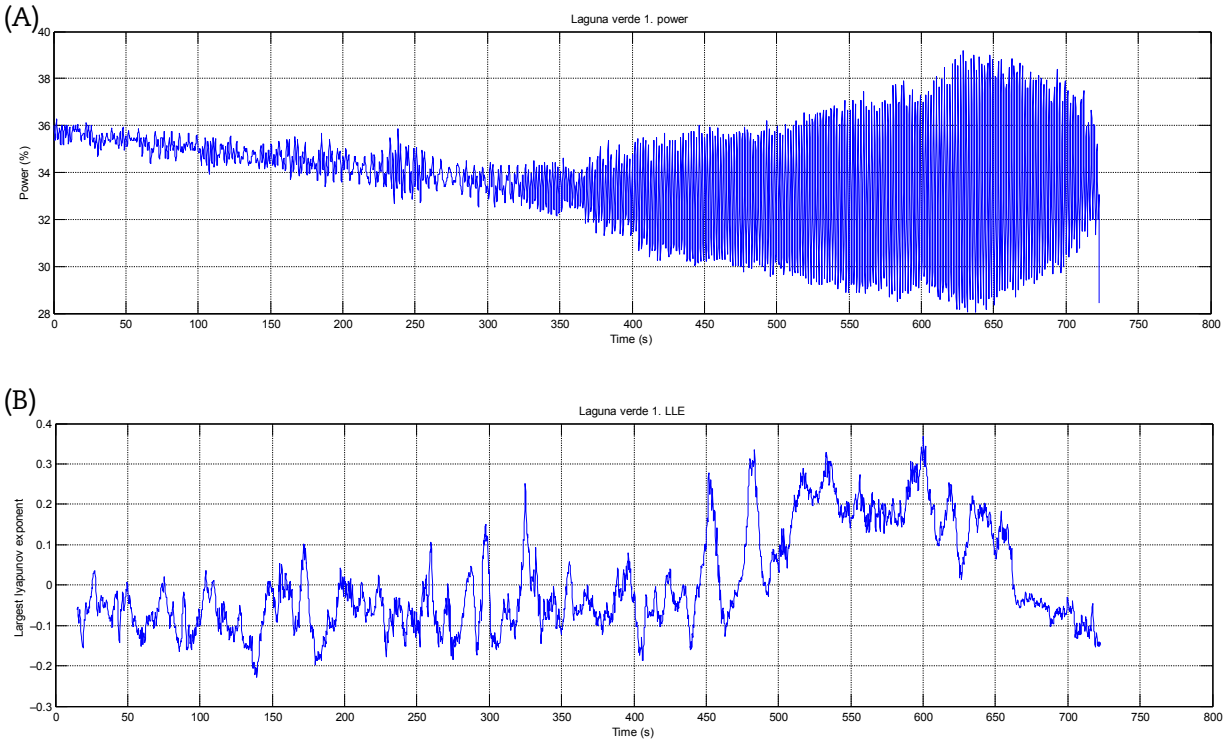

Fig. 12 – Laguna Verde nuclear power plant. (A) Neutronic power series; and (B) LLE(t). LLE, largest Lyapunov exponent.

instabilities have a greater LLE value, as in the case of Forsmark NPP.

The results from the LLE time series calculation methodology uses a rolling window sequence. This analysis sets out partial conclusions that make an interesting use of this technique. Evaluating LLE value in every moment (LLE(*t*)), as well as its tendency, are essential to analyze current and future reactor behavior.

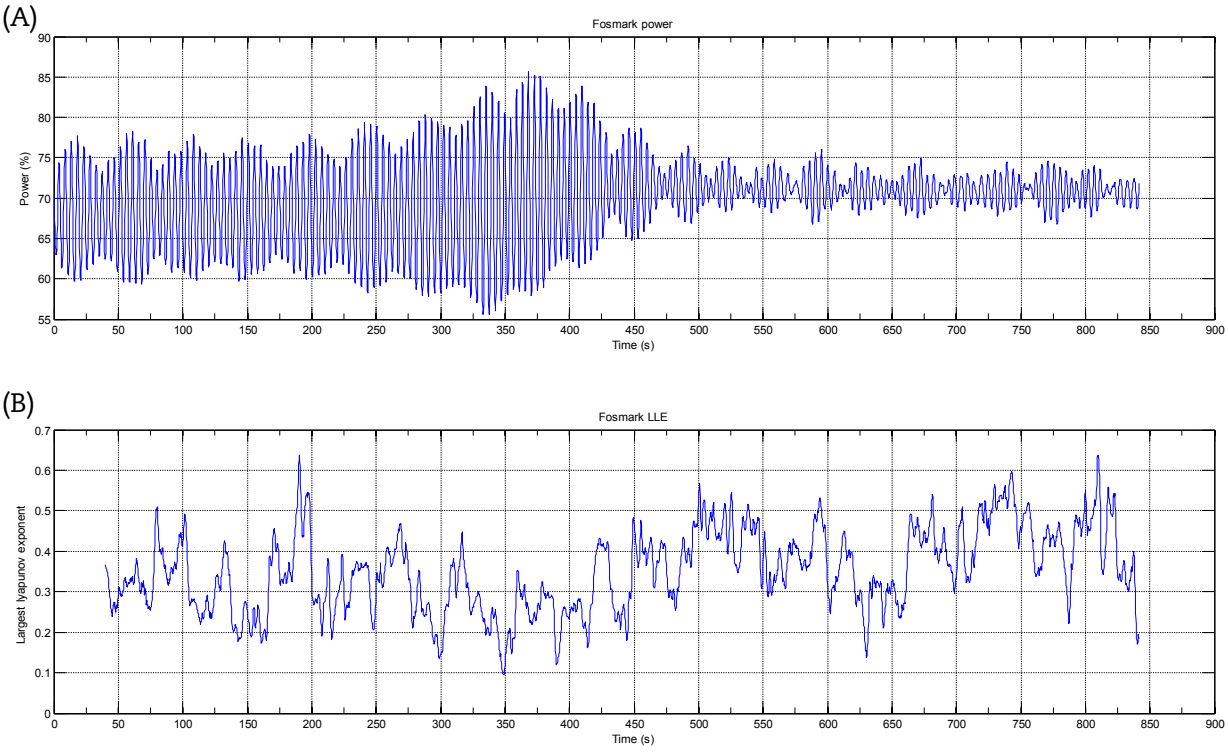

Fig. 13 – Forsmark nuclear power plant. (A) Neutronic power series; and (B) LLE(t). LLE, largest Lyapunov exponent.

Once the meaning of LLE values and their tendency is analyzed, local LLE behavior is analyzed in the positive half-space. This analysis reveals the reversible nature of the system under the situations analyzed. Figs. 11–13 show that when power series respond to a situation of divergence, LLE time series behavior is of the sawtooth type, meaning that the system tends to lose equilibrium. In none of the analyzed cases was the cycle limit exceeded or attraction by the initial equilibrium point. The previous statement justifies the reason presented by March-Leuba et al. [6] in Section 4.4 on density wave instabilities in BWRs.

The attractors constructed from the neutronic power signals are basically the same (isomorphic), because they respond to the same process of neutronic, thermohydraulics, heat transfer, and two-phase flow. The first conclusion is independent of instability type or mode (in-phase and out-of-phase)—the attractor remains similar (Figs. 8–10).

It is also concluded that the system is recoverable, because the elimination of conditions causing instability results in the system returning to its initial situation. This effect is seen in the cases of Cofrentes and Laguna Verde at the end of the series, after the operator acts to address the situation, either by rod insertion or recirculation control valve opening modification.

Conflicts of interest

The authors declare no conflict of interest.

REFERENCES

[1] United States Nuclear Regulatory Commission (U.S. NRC), Power Oscillating in Boiling Water Reactor (BWR5) NRC, Washington (DC), Bulletin No. 88, 1988, p. 7.

[2] J.L. Muñoz-Cobo, G. Verdu, Application of Hopf bifurcation theory and variational methods to the study of limit cycles in boiling water reactors, Ann. Nucl. Energy 18 (1991) 269–302.

[3] C.Y. Yang, N.Z. Cho, Expansion methods for finding nonlinear stability domains of nuclear reactor models, Ann. Nucl. Energy 19 (1992) 347–368.

[4] J.L. Muñoz-Cobo, G. Verdu, C. Pereira, Dynamic reconstruction and Lyapunov exponents from time series data in boiling water reactors, application to BWR stability analysis, Ann. Nucl. Energy 19 (1992) 223–235.

[5] J.P. Eckmann, S. Oliffson, D. Ruelle, S. Ciliberto, Lyapunov exponents from time series, Phys. Rev. A 34 (1986) 4971.

[6] J. March-Leuba, Density-wave Instabilities in Boiling Water Reactors (No. NUREG/CR-6003; ORNL/TM-12130), Nuclear Regulatory Commission, Washington, DC, United States, 1992. Division of Systems Technology; Oak Ridge National Laboratory, Oak Ridge (TN).

[7] C. Pereira, G. Verdú, J.L. Muñoz-Cobo, R. Sanchis, BWR stability from dynamic reconstruction and autoregressive model analysis: application to Cofrentes Nuclear Power Plant, Prog. Nucl. Energy 27 (1992) 51–68.

[8] G. Verdú, D. Ginestar, M.D. Bovea, P. Jiménez, J. Peña, J.L. Muñoz-Cobo, Complex Lyapunov exponents from short and noisy sets of data, Application to stability analysis of BWRs, Ann. Nucl. Energy 24 (1997) 973–994.

[9] H. Konno, S. Kanemoto, Y. Takeuchi, Theory of stochastic bifurcation in BWRs and applications, Prog. Nucl. Energy 43 (2003) 201–207.

[10] T. Suzudo, Application of a nonlinear dynamical descriptor to BWR stability analyses, Prog. Nucl. Energy 43 (2003) 217–223.

[11] G. Verdú, D. Ginestar, J.L. Muñoz-Cobo, J. Navarro-Esbrí, M.J. Palomo, P. Lansaker, J.M. Conde, M. Recio, E. Sartori, Forsmark 1&2 Stability Benchmark. Time Series Analysis Methods for Oscillations during BWR Operation, Final Report, NEA/NSC/DOC, OECD Publications, 2 rue André-Pascal, 75775 PARIS CEDEX 16, 2001, p. 2. Printed in France.

[12] R. Castillo, G. Alonso, J.C. Palacios, Determination of limit cycles using both the slope of correlation integral and dominant Lyapunov methods, Nucl. Technol. 145 (2004) 139–149.

[13] R. Khoda-Bakhsh, S. Behnia, O. Jahanbakhsh, Stability analysis in nuclear reactor using Lyapunov exponent, Ann. Nucl. Energy 35 (2008) 1370–1372.

[14] F.Y. Li, Z. Chen, Y. Liu, Research on stability of a reactor with power reactivity feedback, Prog. Nucl. Energy 67 (2013) 15–17.

[15] C.J. Gavilán Moreno, Use of the HURST exponent as a monitor and predictor of BWR reactor instabilities, Ann. Nucl. Energy 37 (2010) 434–442.

[16] A. Wolf, J.B. Swift, H.L. Swinney, J.A. Vastano, Determining Lyapunov exponents from a time series, Physica D 16 (1985) 285–317.

[17] M.T. Rosenstein, J.J. Collins, C.J. De Luca, A practical method for calculating largest Lyapunov exponents from small data sets, Physica D 65 (1993) 117–134.

[18] S. Sato, M. Sano, Y. Sawada, Practical methods of measuring the generalized dimension and the largest Lyapunov exponent in high dimensional chaotic systems, Prog. Theor. Phys. 77 (1987) 1–5.

[19] H.D. Abarbanel, R. Brown, J.J. Sidorowich, L.S. Tsimring, The analysis of observed chaotic data in physical systems, Rev. Mod. Phys. 65 (1993) 1331.

[20] H.D. Abarbanel, M.B. Kennel, Local false nearest neighbors and dynamical dimensions from observed chaotic data, Phys. Rev. E 47 (1993) 3057.

[21] United States Nuclear Regulatory Commission (U.S. NRC), Density-wave Instabilities in Boiling Water Reactors, Oak Ridge National Laboratory, Oak Ridge (TN), 1992. NUREG/CR-6003 ORNL/TM-12130.

[22] R. Castillo, G. Alonso, J.R. Ramírez, Validation of SIMULATE-3K for stability analysis of Laguna Verde nuclear plant, Nucl. Eng. Des. 265 (2013) 19–24.

[23] R. Castillo, J.R. Ramírez, G. Alonso, J. Ortiz-Villafuerte, Prony's method application for BWR instabilities characterization, Nucl. Eng. Des. 284 (2015) 67–73.

[24] C.J. Gavilan Moreno, A. Prieto-Guerrero, G. Espinosa-Paredes, Nuclear power plant instabilities analysis, Ann. Nucl. Energ 85 (2015) 279–289.

[25] L. Noakes, The Takens embedding theorem, Int. J. Bifurcation Chaos 1 (1991) 867–872.

[26] F. Takens, Detecting Strange Attractors in Turbulence, Springer, Berlin, 1981, pp. 366–381.

[27] H.L. Swinney, Independent coordinates for strange attractors from mutual information, Phys. Rev. A 33 (1986) 1134–1140.

[28] M. Small, Applied Nonlinear Time Series Analysis: Applications in Physics, Physiology and Finance, Vol. 52, Nonlinear Science Series A, World Scientific, Singapore, 2005.

[29] L.D. Iasemidis, J.C. Sackellares, The evolution with time of the spatial distribution of the largest Lyapunov exponent on the human epileptic cortex, in: D.W. Duke, W.S. Pritchard

(Eds.), Measuring Chaos in the Human Brain, World Scientific, Singapore, 1991, pp. 49–82.
[30] A. Komori, T. Baba, T. Morisaki, M. Kono, H. Iguchi, K. Nishimura, K. Matsuok, Correlation dimension and largest Lyapunov exponent for broadband edge turbulence in the compact helical system, Phys. Rev. Lett. 73 (1994) 660.
[31] A.D. Krystal, C. Zaidman, H.S. Greenside, R.D. Weiner, C.E. Coffey, The largest Lyapunov exponent of the EEG during ECT seizures as a measure of ECT seizure adequacy, Electroencephalogr. Clin. Neurophysiol. 103 (1997) 599–606.
[32] A. Torcini, R. Livi, A. Politi, S. Ruffo, Comment on universal scaling law for the largest Lyapunov exponent in coupled map lattices, Phys. Rev. Lett. 78 (1997) 1391.
[33] R. Van Zon, H. Van Beijeren, C. Dellago, Largest Lyapunov exponent for many particle systems at low densities, Phys. Rev. Lett. 80 (1998) 2035.
[34] A. Giovanni, M. Ouaknine, J.M. Triglia, Determination of largest Lyapunov exponents of vocal signal: application to unilateral laryngeal paralysis, J. Voice 13 (1999) 341–354.
[35] A. Stefanski, Estimation of the largest Lyapunov exponent in systems with impacts, Chaos Solitons Fract. 11 (2000) 2443–2451.
[36] K.E. Chlouverakis, M.J. Adams, Stability maps of injection-locked laser diodes using the largest Lyapunov exponent, Opt. Commun. 216 (2003) 405–412.